JOURNAL OF BACTERIOLOGY, Aug. 1998, p. 3940–3945 Vol. 180, No. 15
0021-9193/98/$04.00+0

Identification of an Intragenic Ribosome Binding Site That Affects Expression of the *uncB* Gene of the *Escherichia coli* Proton-Translocating ATPase (*unc*) Operon

SHARLENE R. MATTEN,[1]† THOMAS D. SCHNEIDER,[2] STEVEN RINGQUIST,[3]‡ AND WILLIAM S. A. BRUSILOW[1]*

Department of Biochemistry and Molecular Biology, Wayne State University School of Medicine, Detroit, Michigan 48201[1]; Laboratory of Computational and Experimental Biology, National Cancer Institute, Frederick, Maryland 21702-1201[2]; and Department of Molecular, Cellular, and Developmental Biology, University of Colorado, Boulder, Colorado 80309[3]

Received 7 August 1997/Accepted 1 June 1998

The *uncB* gene codes for the a subunit of the F_o proton channel sector of the *Escherichia coli* F_1 F_o ATPase. Control of expression of *uncB* appears to be exerted at some step after translational initiation. Sequence analysis by the perceptron matrices (G. D. Stormo, T. D. Schneider, L. Gold, and A. Ehrenfeucht, Nucleic Acids Res. 10:2997–3011, 1982) identified a potential ribosome binding site within the *uncB* reading frame preceding a five-codon reading frame which is shifted one base relative to the *uncB* reading frame. Elimination of this binding site by mutagenesis resulted in a four- to fivefold increase in expression of an *uncB′-′lacZ* fusion gene containing most of *uncB*. Primer extension inhibition (toeprint) analysis to measure ribosome binding demonstrated that ribosomes could form an initiation complex at this alternative start site. Two fusions of *lacZ* to the alternative reading frame demonstrated that this site is recognized by ribosomes in vivo. The results suggest that expression of *uncB* is reduced by translational frameshifting and/or a translational false start at this site within the *uncB* reading frame.

The *Escherichia coli unc* (also called *atp*) operon is comprised of nine genes which encode the subunits of the proton-translocating F_1F_o ATPase. This enzyme couples an electrochemical gradient of protons to the synthesis of ATP from ADP and P_i. Under anaerobic conditions, the enzyme hydrolyzes ATP and pumps protons across the cytoplasmic membrane to form a proton gradient which can be used in the uptake of essential nutrients such as sugars and amino acids. The nine genes of the *unc* operon are transcribed in the order *uncIBEFHAGDC*, corresponding to protein i, which has no known function, and subunits a, c, b, δ, α, γ, β, and ε. These subunits are integrated into two sectors, the F_o and the F_1. The F_o is the proton-conducting integral membrane sector composed of the a, b, and c subunits. The F_1 is the peripheral sector carrying the catalytic sites for ATP synthesis and hydrolysis (for reviews, see references 6, 18, and 23). Each gene exists in a single copy within the operon, and the operon is transcribed into a single polycistronic mRNA, yet the subunits encoded by these genes exist in different numbers in the assembled complex. It has been shown that differences in translational initiation result in differential synthesis of many of the subunits (15).

Particularly interesting is the stoichiometry of the a and c subunits of the F_o sector, encoded by *uncB* and *uncE*, respectively. The a/c ratio in the assembled complex has been determined to be 1:10 (5), and it is clear that in a variety of experiments, the a and c subunits are synthesized in significantly different amounts (2, 19). However, our previous studies on expression of a series of *uncB′-′lacZ* fusion genes (25) demonstrated that translational initiation of *uncB* is apparently as efficient as initiation of *uncE* (c subunit). Early fusions, containing 10 to 15% of *uncB* fused to *lacZ*, produced as much β-galactosidase activity as an *uncE′-′lacZ* fusion. A late *uncB′-′*lacZ fusion, carrying about 95% of *uncB*, however, was expressed 10 times less well than the early fusions. Also, Lang et al. (14) showed that even though the a and c subunits were synthesized in vitro at significantly different rates, ribosome binding to *uncB* appeared to be very similar to that of *uncE*, especially when the ratio of mRNA to ribosomes was low. The *uncB* reading frame might therefore contain some posttranslational initiation signals which decrease synthesis of the a subunit. The present study analyzed the *uncB* reading frame for alternative ribosome recognition sites and tested the hypothesis that *uncB* expression is influenced by the presence of such a site.

MATERIALS AND METHODS

Plasmids. Plasmids pDKWH103, pKS104, and pKS105 were described previously (25). Plasmid pSRM106 is identical to pKS104 except for the T→C mutation at position 285 of *uncB*, as shown below (see Fig. 2). The 617-bp *Bam*HI fragment within *uncB* was cloned into M13 and mutagenized to change the false start ATG codon to ACG, by using the mutagenic primer 5′-GCTTTTGCCGT GGTACATGTC-3′. The entire fragment was sequenced to ensure that there were no additional mutations. The mutagenized fragment was then used to construct pSRM106 just as the wild-type fragment had been used to construct pKS104 (25). Plasmid pSRM114 was constructed by mutagenizing the 617-bp *Bam*HI fragment so that the termination codon of the false start reading frame was eliminated, and the false start reading frame was fused in frame to the *uncB* reading frame. The mutagenic primer 5′-GGCCAGCGGAGCAATGCTTGCT TTTGCCATG-3′ results in the deletion of the first two bases, TG, of the stop codon for the false start reading frame. Plasmid pWSB52 consists of *lacZ* fused directly to the false start initiation codon. An *Nco*I site was added to the *lac* fusion vector pMLB1034 (24) by digesting the plasmid with *Eco*RI and ligating

* Corresponding author. Mailing address: Department of Biochemistry and Molecular Biology, Wayne State University School of Medicine, Scott Hall, 540 E. Canfield Ave., Detroit, MI 48201. Phone: (313) 577-6659. Fax: (313) 577-2765. E-mail: wbrusilow@med.wayne.edu.

† Present address: U.S. Environmental Protection Agency, Washington, DC 20460.

‡ Present address: Sidney Kimmel Cancer Center, San Diego, CA 92121.

in the presence of an *Eco*RI-*Nco*I adaptor, 5′-AATTCCCATGGG-3′. The resultant plasmid, pWSB53, contained an *Nco*I site, the ATG for which is in frame with *lacZ*. The false start initiation codon was then cloned into this vector by digesting pKS104 with *Pst*I and *Nco*I and cloning the resultant fragment into pWSB53 which had been digested with *Pst*I and *Nco*I. The resultant plasmid, pWSB52, carries the *unc* promoter, *uncI*, and *uncB* up to the false start initiation codon, the ATG for which is part of the *Nco*I site, and is in frame with the *lacZ* gene of pMLB1034.

Assays of β-galactosidase activity. As described by Solomon et al. (25), these fusions were constructed in plasmids and then recombined into λ and finally into the λ *att* site to create single-copy fusions in the chromosome of MC1000 Δ(*uncI-uncC*), an *E. coli* strain deleted for both *unc* and *lac* (1). β-Galactosidase activities produced by each fusion gene in single-copy lysogens were assayed as described by Miller (17). The values for the β-galactosidase activities produced by single copies of the fusions in pDKWH103 and pKS105 are from the work of Solomon et al. (25).

Toeprint analysis. Primer extension inhibition (toeprint) analysis of the intragenic false start site within *uncB* was performed. The extent of ribosome binding in the initiation region of protein synthesis was determined by primer extension inhibition. RNA was synthesized in vitro from PCR-generated DNA. Primers containing the T7 polymerase promoter sequence and DNA flanking the false start site were used to mutagenize the sequence. T7 polymerase was then used to synthesize RNA. The transcript was purified on a 6% acrylamide gel and annealed to a ^{32}P-end-labeled oligonucleotide primer (see Fig. 3); this was followed by RNA sequencing reactions and primer extension inhibition (toeprinting) reactions without and with 30S ribosomes and $tRNA^{fMet}$, as described by Hartz et al. (8), except that gel-purified RNA was used. Toeprinting reaction mixtures contained 100 nM 30S subunits and 500 nM $tRNA^{fMet}$. Preincubation was done for 10 min at 37°C; this was followed by primer extension for 15 min at 37°C with Moloney murine leukemia virus reverse transcriptase (200 U/reaction mixture).

Immunoblots of fusion proteins. *E. coli* MC1000 Δ(*uncI-uncC*) (1) carrying either pKS104, pSRM114, or pWSB52 was grown in LB-ampicillin medium to an optical density at 600 nm of 0.4 to 0.7 and then chilled, pelleted by centrifugation, resuspended in 3 ml of 10 mM MOPS (morpholinepropanesulfonic acid)–10 mM $MgCl_2$ (pH 7), and lysed in a French press at 16,000 lb/in^2. The pKS104 culture was grown in 25 ml of medium; the other two were grown in 250 ml. Unlysed cells were removed by centrifugation, and the supernatant fractions were loaded onto a sodium dodecyl sulfate (SDS)–7% polyacrylamide gel. Electrophoresis and immunoblotting, with anti-β-galactosidase (Promega Corporation, Madison, Wis.), were carried out as described previously (3).

TABLE 1. Perceptron analysis of the *unc* operon[a]

Nucleotide position[b]	Weight matrix score[c]			Gene name[d]
	w51	w71	w101	
374	−76	39	−59	
623	−199	−94	−108	*uncI*
708	−53	8	96	
1024	13	35	21	*uncB*
1307	36	62	61	—[e]
1886	131	−72	−152	*uncE*
1901	40	−62	−151	
2187	−326	−267	−155	*uncF*
2261	−62	45	−48	
2672	57	132	196	*uncH*
2801	−128	−62	22	
2919	24	−127	−99	
3143	−50	21	−111	
3218	365	212	42	*uncA*
3443	113	−112	−170	
3736	−268	−225	15	
4524	5	−33	−184	
4810	6	−14	−12	*uncG*
5700	329	155	69	*uncD*
7103	175	124	98	*uncC*

[a] The ECOUNC entry (accession no. J01594) was obtained from GenBank and searched by the three perceptron matrices (26). The matrices had not been trained on this sequence.

[b] Nucleotide position from ECOUNC for each ATPase gene initiation codon or any sequence which produced a positive score in the perceptron matrix analysis.

[c] Scores produced by analysis of each nucleotide position with each of the three matrices, w51, w71, and w101.

[d] ATPase gene whose initiation codon corresponds to the given position.

[e] —, position identified by all three matrices but not corresponding to any one of the known translational initiation sites.

RESULTS

Potential ribosome binding sites of the entire *unc* sequence, including *uncB*, were distinguished from other sites by using three perceptron weight matrices developed previously, w101, w71, and w51 (26). Each perceptron weight matrix represents a ribosome as it scans the mRNA. Translational initiation occurs with some fixed probability at any site along the RNA message. This probability is related to the value given by the perceptron weight matrix when positioned at a given site. Regions with a proper initiation codon and Shine-Dalgarno sequence are given positive values by the perceptron weight matrices. A higher weight matrix score indicates that a particular sequence fitting within the bounds of the chosen matrix is more likely to be a ribosome binding site. The results of this analysis of the *unc* operon are shown in Table 1. All three matrices identified ribosome binding sites (i.e., produced positive values) at the initiation codons for *uncB*, *-H*, *-A*, *-D*, and *-C*. One matrix identified the initiation codon for *uncE*. None of the matrices identified ribosome binding sites preceding *uncI* or *uncF*. Other potential ribosome binding sites are indicated by positive values in the table. All three matrices identified a site within *uncB* (at base 1307) as being a potential ribosome binding site. Figure 1 shows the location of this potential false start and how the resultant reading frame is five codons long and shifted one base compared to the *uncB* reading frame. Except for this site and the true initiation codons for five of the ATPase genes, no other site in the operon was given a positive score by all three matrices.

Effect of mutagenizing the false start ribosome binding site on expression of the late *uncB′-′lacZ* fusion gene. As discussed above, even though the differential expression of most of the ATPase genes appears to be controlled at the level of translational initiation, past studies suggest that synthesis of the a subunit is controlled at some step after initiation. We tested the role of the alternative reading frame identified by perceptron analysis in decreasing the expression of the pKS104 *uncB′-′lacZ* fusion gene, which contains most of the *uncB* gene (25) (Fig. 2). The CAU corresponding to histidine-95 (Fig. 1) was changed to a CAC (also histidine), creating plasmid pSRM106. This mutation converted the false-start AUG to ACG, thereby destroying the putative ribosome binding site. The score resulting from perceptron w101 analysis of this region changed from +61 to −69 as a result of this single change. The scores resulting from analysis by the other matrices were even more negative. Eliminating this false start ribosome binding site resulted in a four- to fivefold increase in expression of the *uncB′-′lacZ* fusion gene from 10 to 12 U of β-galactosidase for the unmutated single-copy KS104 construction to 45 to 50 U for the mutated single-copy SRM106 fusion gene. Mutation of the site identified by perceptron analysis increases expression of *uncB* (Fig. 2).

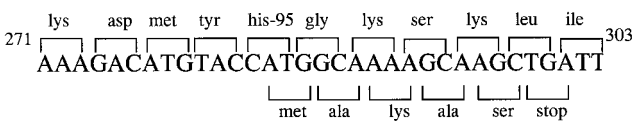

FIG. 1. Location of translation false start within *uncB*. All three perceptron weight matrices identified this region as a translation initiation region. The bases between positions 271 and 303 of the *uncB* reading frame are shown. The amino acids of the *uncB* product coded for by those bases are shown above them. The false start translation initiation site identified by the perceptron matrices, followed by a short reading frame, is indicated below the bases.

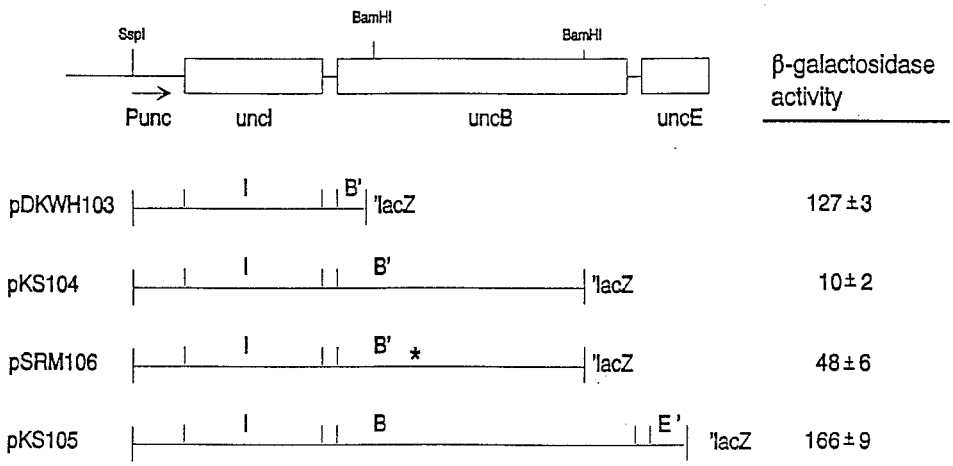

FIG. 2. β-Galactosidase activities produced by in-frame *uncB'-'lacZ* fusions. Locations of the *unc* promoter (P_{unc}), *uncI*, *uncB*, and *uncE* are shown at the top of the figure. The amounts of *unc* DNA fused in frame to *lacZ* in plasmids pDKWH103, pKS104, and pKS105 are indicated by the horizontal lines. Plasmid pSRM106 is identical to pKS104 except for the T→C mutation at position 285 of *uncB*, which is indicated by an asterisk. β-Galactosidase activities produced by each fusion gene in single-copy lysogens were assayed as described by Miller (17). The values for the β-galactosidase activities produced by single copies of the fusions in pDKWH103 and pKS105 are from the work of Solomon et al. (25).

Toeprint analysis of the false start ribosome binding site. To determine whether this false start region was actually capable of forming an initiation complex with ribosomes and initiator tRNA, we carried out primer extension inhibition experiments, also called toeprint analysis (8). In a toeprint experiment, reverse transcriptase is allowed to begin transcribing an mRNA from a primer downstream of a putative ribosome binding site. Without ribosomes in the reaction mixture, the reverse transcriptase should pass across the site. When ribosomes are included and allowed to bind, they block the transcriptase, and a distinct band forms 15 bases downstream of the initiation codon. Such analysis has been done previously for the ribosome binding sites of the genes of the *unc* operon (22).

In our initial studies on the mRNA produced by the pKS104 plasmid, which consists of the true *unc* promoter, *uncI*, and most of *uncB* fused in frame to *lacZ* (Fig. 2), we detected no toeprint at the false start. Computer analysis of the mRNA around the false start suggested the existence of a strong secondary structure (Fig. 3) which, in the in vitro toeprint experiment, might prevent or interfere with ribosome binding. A smaller stem-loop structure immediately following the larger stem-loop might also interfere with the primer extension reaction used to create the toeprint (Fig. 3). Using mutagenic PCR primers, we replaced 21 bases of one side of the stem-loop with 11 adenosine residues, and we made three single base changes in the smaller stem-loop to minimize its effect on the primer extension reactions (Fig. 3). Ribosome binding to the resultant mRNA revealed a strong toeprint +15 bases from the false start initiation codon, precisely where the perceptron analysis predicted it (Fig. 4). Therefore, this region is capable of forming an initiation complex with ribosomes once the mRNA secondary structure is disrupted.

The RNA synthesized for the toeprint analysis was too short in sequence to be analyzed by any of the perceptron weight matrices. To evaluate how these mutations might affect the perceptron analysis, we assumed the presence of 100 adenosine residues on each end of the sequence, analyzed those sequences with the perceptron matrices, and found that the changes which allowed us to observe a toeprint were changes which raised the perceptron score resulting from analysis with the w51 matrix but lowered the scores resulting from analysis with the other two matrices. It is therefore unlikely that these mutations were creating a new ribosome binding site. Interestingly, analysis of the mutated sequence by the w51 matrix gave a positive score to a site seven bases upstream of the false start

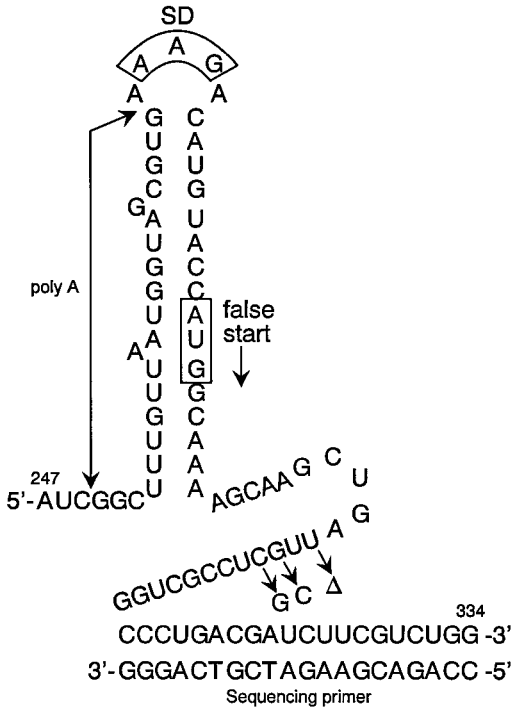

FIG. 3. Putative mRNA secondary structure around translational false start. The sequence between bases 247 and 334 of *uncB* are shown folded into a secondary structure predicted by the MFOLD program, version 2.0 (10, 11, 30). The false-start AUG and the primer used for sequencing and for primer extension in the toeprint experiment are indicated. To obtain a toeprint of this site, the region indicated by the arrows was replaced by 11 adenosine residues, and a single-base deletion and two single-base mutations were constructed in the small loop, as indicated.

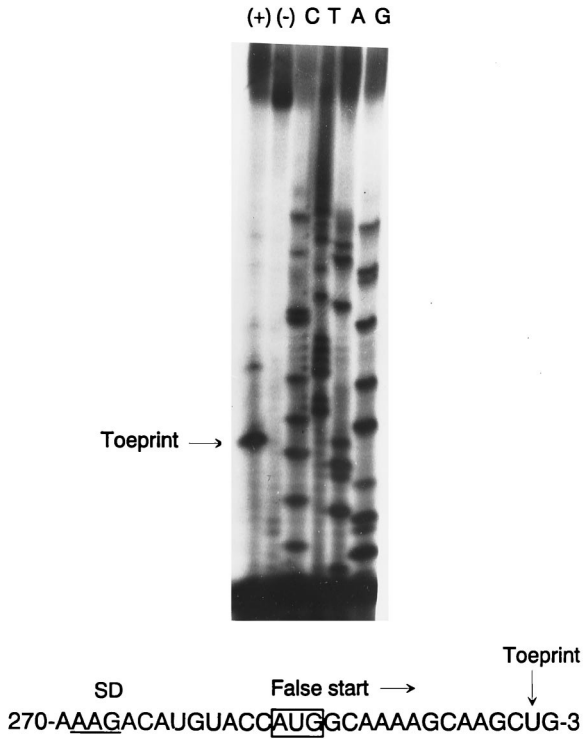

FIG. 4. Primer extension inhibition (toeprint) analysis of the intragenic false start site within *uncB*. The extent of ribosome binding in the initiation region of protein synthesis was determined by primer extension inhibition as described in Materials and Methods. Sequencing lanes (G, A, T, and C) are indicated. Lanes labeled (+) and (−) represent reactions run in the presence or absence of ribosomes, respectively. Next to lane (+), an arrow indicates the toeprint band which forms at +15 from the false start initiation codon. Below the autoradiogram is shown the location of the toeprint within the initiation domain of the false start, 15 nucleotides 3′ of the first base of the initiation codon AUG (boxed). The Shine-Dalgarno sequence (SD) is underlined. The band seven bases above the toeprint could be a minor ribosome binding region predicted by the w51 matrix (see Results).

site, and the primer extension inhibition analysis (Fig. 4) revealed a minor toeprint at that site.

Translational initiation at the false start. We fused *lacZ* to the false start reading frame two ways (Fig. 5). First, we deleted the first two bases, TG, of the stop codon of the false start reading frame so that this reading frame, instead of ending, was fused to the remainder of the *uncB* reading frame. The resultant plasmid, pSRM114, is therefore identical to pKS104 except for a mutation which disrupts the true *uncB* reading frame at the stop codon for the false start reading frame. Second, we fused *lacZ* in frame directly to the false start initiation codon to create pWSB52. β-Galactosidase activity produced by either of these two constructions probably results either from translation initiation at the false start or ribosomal frameshifting at the false start. We compared the β-galactosidase activities produced in *unc*-deleted cells carrying pKS104, pSRM114, or pWSB52. The true *uncB′-′lacZ* fusion plasmid pKS104 produces between 200 and 600 U of activity in cells grown on minimal medium containing antibiotic. (Measurements of activity produced by high-copy-number plasmids produce a much wider range of activities than those produced by single-copy lysogens.) Cells carrying plasmid pSRM114 produce 10 to 20 U, and cells carrying pWSB52 produce 50 to 60 U under the same conditions. When the false start codon in pWSB52 was mutagenized to an ACG, the β-galactosidase activity produced from the resultant multicopy plasmid dropped by an average of 70%. Although this decrease confirms that translation is initiated at this site, the fact that activity was not completely abolished indicates that additional factors contribute substantially to ribosome frameshifting and/or reinitiation at this site.

When the fusion in pWSB52 was moved into λ to create single-copy lysogens, it produced very low but non-zero activity in our normal assay, approximately 5 to 10% of the activity produced by the λpKS104 lysogen. The single-copy activity produced from the SRM114 construction was too low to measure.

As a further demonstration that ribosomes recognize the false start site in vivo, we analyzed whole-cell lysates of MC1000 Δ(*uncI-uncC*) carrying the three fusion plasmids pKS104, pSRM114, and pWSB52 by immunoblotting with anti-β-galactosidase (Promega). The results are shown in Fig. 6. Lane 1 contains the products of pKS104. The full-length *uncB′-′lacZ* product is clearly visible as the highest-molecular-weight band. As is often observed with β-galactosidase fusion proteins, all three lysates contain a significant amount of the β-galactosidase moiety alone, which probably results from proteolysis at or near the fusion joint. Lane 2 contains the products of pSRM114. The product visible as the top band, which is the same size as the fusion protein produced by pKS104, could be produced only by translational initiation at the true *uncB* start codon and ribosomal frameshifting in the vicinity of the false start reading frame. Compared to pKS104, pSRM114 also produces an additional fusion protein (lane 2). This additional protein is the correct size for a fusion protein that was initiated at the false start initiation codon. Since this band is not visible at all in the products of pKS104, it is unlikely to be a proteolysis product of the full-length fusion protein. The fusion protein made from pWSB52 (lane 3) would be the same size as the β-galactosidase moiety produced by cleavage at the fusion joint of the other full-length fusion proteins, if translation were to initiate at the false start. The higher-molecular-weight protein produced by pWSB52 (lane 3) is the correct size for the product of the true *uncB* translational start site frameshifted at the false start. The relatively small difference in molecular weight between this frameshifted protein produced by pWSB52 and the protein initiating at the false start in pSRM114 would not be detectable on these gels (~5,500 difference in proteins with

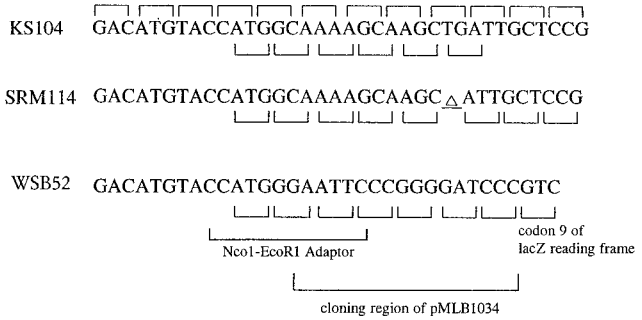

FIG. 5. Plasmid constructions which fuse *lacZ* to the false start reading frame. The top line shows the unmutagenized region of the false start in the *uncB′-′lacZ* fusion gene found in pKS104 (see Fig. 1 and 2 for more detail). In plasmid pSRM114, the termination codon of the false start reading frame is eliminated, and the false start reading frame is fused in frame to the *uncB* reading frame. Plasmid pWSB52 consists of *lacZ* fused directly to the false start initiation codon. The details of these constructions are given in Materials and Methods. Ribosomes initiating at the true *uncB* initiation codon terminate 31 codons downstream of the deletion in pSRM114 and 6 codons after the indicated sequence in pWSB52.

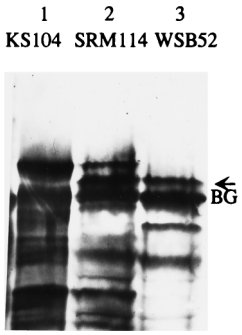

FIG. 6. Immunoblots of fusion proteins. Lysates were prepared from *E. coli* MC1000 Δ (*uncI-uncC*) (1) carrying either pKS104, pSRM114, or pWSB52 as described in Materials and Methods. The pKS104 culture was grown in a 25-ml volume; the other two were grown in 250 ml. Unlysed cells were removed by centrifugation, and the supernatant fractions were loaded onto an SDS–7% polyacrylamide gel. Electrophoresis and immunoblotting, with anti-β-galactosidase (Promega), were carried out as described previously (3). The samples and amounts loaded were as follows: pKS104, 12 μg (lane 1); pSRM114, 250 μg (lane 2); pWSB52, 250 μg (lane 3). Lanes 2 and 3 therefore contained 20 times as much total protein as lane 1. The top band in lane 1 is the full-length fusion protein coded for by pKS104; it consists of most of the a subunit fused in frame to β-galactosidase. The top band in lane 2 is the same-size protein, which could result only from a frameshift at the false start of ribosomes which had initiated at the true *uncB* translation start site. The second band (arrow) in lane 2 represents a *lac* fusion protein initiated at the false start site. The top band (arrow) in lane 3 is the proper size for a protein initiated at the true *uncB* translational start site and fused to *lacZ* by frameshifting at the false start. The second bands in lanes 1 and 2 represent the β-galactosidase moiety (BG) derived from proteolysis of each fusion protein at the fusion joint. The equivalent band in lane 3 probably represents the fusion protein derived from translational initiation at the false start together with the β-galactosidase moiety derived from proteolysis of the higher-molecular-weight fusion protein at the fusion joint.

a molecular weight of >125,000), especially considering that the a subunit is known to migrate anomalously in SDS gels. These results support the conclusion that ribosomes can recognize the false start site in vivo and that this site probably produces both ribosomal frameshifting and translational initiation.

DISCUSSION

The *uncB* gene codes for the a subunit, which is present in 1 copy per ATPase complex. This subunit is the most complex transmembrane subunit in the F_o, and several residues are believed to be involved in proton translocation across the membrane (23, 27). However, the a subunit alone has been demonstrated to be harmful to growing cells. Overexpression of *uncB* has been shown to have deleterious effects on cell growth (12, 28). Studies on expression of the first three genes of the operon have shown that the a subunit is synthesized more poorly than the c subunit, which is encoded by *uncE*, even though translation initiation levels of *uncB* and *uncE* appear to be comparable (14, 25). The relatively low rate of expression of *uncB* is not well understood. Studies of the *unc* transcript have shown that the mRNA transcript within the *uncB* cistron is more sensitive to cleavage and degradation than most of the genes in the operon (13, 16, 20, 21), so even though *uncB* is preceded by a relatively strong translation initiation region, the presence of sites of endonucleolytic attack, leading to specific mRNA degradation, might be responsible for the relatively low level of synthesis of the a subunit. Additionally, we have shown that the mysterious *uncI* gene also plays a posttranslation initiation role in controlling expression of *uncB* (9). The studies described here suggest an additional or alternative control mechanism to explain the relatively low level of synthesis of the a subunit despite its apparent high rate of translational initiation. Perceptron matrices were trained to analyze nucleotide sequences for potential ribosome binding sites. Analysis of the *unc* operon by these matrices identified a potential strong ribosome binding site within *uncB*, frameshifted one base relative to the *uncB* reading frame. Elimination of the false start AUG at this internal ribosome binding site resulted in increased expression of the late *uncB′-′lacZ* fusion gene, so this site clearly has a significant effect on *uncB* expression, even though its elimination does not increase expression of the KS104 fusion to the level measured for the DKWH103 fusion. Both the CAC and CAU histidine codons are present with equal frequencies in *E. coli* genes (29), so the effect probably does not result from altered codon usage. The experiments presented here demonstrate that this region is capable of forming an initiation complex with ribosomes, although it was necessary to mutagenize the mRNA secondary structure around this site before such an in vitro complex could be observed. Finally, fusing this alternative ribosome binding site to *lacZ* in frame produced β-galactosidase activity in vivo from multicopy plasmids, and immunoblot analysis of the resultant fusion proteins shows that both ribosomal frameshifting and translational initiation occur at the false start.

This ribosome binding site obviously exerts some effect on the expression of *uncB*, and it appears to do so through recognition by ribosomes. These studies do not address the mechanism of action of this site, although we can speculate that ribosomes stall at this site due to either the frameshifted ribosome binding site, the mRNA secondary structure, or both. No toeprint is observed on RNA carrying the wild type sequence, so it is unlikely that unbound ribosomes initiate translation at this site. The low rate of expression of *lac* fusions to the false start ribosome binding site also indicates that ribosomes frameshift and initiate translation at this site poorly. The effect of this site on *uncB* expression may involve a relationship between translation and mRNA breakdown. The *uncB* mRNA has been shown to be more susceptible to degradation than other cistrons in the operon (13, 16, 20, 21). It has been demonstrated by Chevrier-Miller et al. (4) that uncoupling of transcription and translation leads to differential mRNA half-lives of *lacZ* mRNA. These authors proposed that inefficient ribosome loading might unwind the RNA without protecting it, making such RNA less stable than untranslated RNA. In studies of RNaseE cleavage of mRNA, Gross (7) has speculated that RNase recognition of mRNA requires some undefined interactions of mRNA with ribosomes, so that only translated mRNA is susceptible to degradation. It is therefore possible that the translational false start identified in these experiments might affect either the number of ribosomes that complete the translation of *uncB*, the sensitivity of the *uncB* message to endonucleolytic degradation, or both.

ACKNOWLEDGMENTS

This research was supported by National Science Foundation grant DMB-9096159 and by American Heart Association grant-in-aid 93007730. S.R.M. was supported by grant 7620010 from the American Heart Association, Maryland Affiliate.

We thank Heven Sze of the Department of Botany and Tomas Kempe of the Protein and Nucleic Acid Synthesis Laboratory, both at the University of Maryland. We also thank Larry Gold of the Department of Molecular, Cellular, and Developmental Biology at the University of Colorado for the use of his laboratory for the toeprinting and Robert Traut of the University of California, Davis, for generously providing purified 30S ribosomes.

REFERENCES

1. **Angov, E., and W. S. A. Brusilow.** 1988. Use of *lac* fusions to measure in vivo regulation of expression of *Escherichia coli* proton-translocating ATPase

(*unc*) genes. J. Bacteriol. **170:**459–462.
2. **Brusilow, W. S. A., D. J. Klionsky, and R. D. Simoni.** 1982. Differential polypeptide synthesis of the proton-translocating ATPase of *Escherichia coli*. J. Bacteriol. **151:**1363–1371.
3. **Brusilow, W. S. A.** 1987. Proton leakiness caused by cloned genes for the F_o sector of the proton-translocating ATPase of *Escherichia coli*. J. Bacteriol. **169:**4984–4990.
4. **Chevrier-Miller, M., N. Jacques, O. Raibaud, and M. Dreyfus.** 1990. Transcription of single-copy hybrid *lacZ* genes by T7 RNA polymerase in *Escherichia coli*: mRNA synthesis and degradation can be uncoupled from translation. Nucleic Acids Res. **18:**5787–5792.
5. **Foster, D. L., and R. H. Fillingame.** 1982. Stoichiometry of subunits in the H^+-ATPase complex of *Escherichia coli*. J. Biol. Chem. **257:**2009–2015.
6. **Futai, M., T. Noumi, and M. Maeda.** 1989. ATP synthase (H^+-ATPase): results by combined biochemical and molecular biological approaches. Annu. Rev. Biochem. **58:**111–136.
7. **Gross, G.** 1991. RNaseE cleavage in the *atpE* leader region of *atpE*/interferon-β hybrid transcript in *Escherichia coli* causes enhanced rates of mRNA decay. J. Biol. Chem. **266:**17880–17884.
8. **Hartz, D., D. S. McPheeters, and L. Gold.** 1989. Selection of the initiator tRNA by *Escherichia coli* initiation factors. Genes Dev. **3:**1899–1912.
9. **Hsu, D. K. W., and W. S. A. Brusilow.** 1995. Effects of uncI on expression of uncB, the gene coding for the a subunit of the F_1F_o ATPase of *Escherichia coli*. FEBS Lett. **371:**127–131.
10. **Jaeger, J. A., D. H. Turner, and M. Zucker.** 1989. Improved predictions of secondary structures for RNA. Proc. Natl. Acad. Sci. USA **86:**7706–7710.
11. **Jaeger, J. A., D. H. Turner, and M. Zucker.** 1990. Predicting optimal and suboptimal secondary structures for RNA. Methods Enzymol. **183:**281–306.
12. **Kanazawa, H., T. Kiyasu, T. Noumi, and M. Futai.** 1984. Overproduction of subunit a of the F_o component of proton-translocating ATPase inhibits growth of *Escherichia coli* cells. J. Bacteriol. **158:**300–306.
13. **Lagoni, O. R., K. von Meyenberg, and O. Michelsen.** 1993. Limited differential mRNA inactivation in the *atp* (*unc*) operon of *Escherichia coli*. J. Bacteriol. **175:**5791–5797.
14. **Lang, V., C. Gualerzi, and J. E. G. McCarthy.** 1989. Ribosomal affinity and translational initiation in *Escherichia coli*. J. Mol. Biol. **210:**659–663.
15. **McCarthy, J. E. G., and C. Bokelman.** 1988. Determinants of translational initiation efficiency in the *atp* operon of *Escherichia coli*. Mol. Microbiol. **2:**455–465.
16. **McCarthy, J. E. G., B. Gerstel, B. Surin, U. Wiedeman, and P. Ziemke.** 1991. Differential gene expression from the *Escherichia coli atp* operon mediated by segmental differences in mRNA stability. Mol. Microbiol. **5:**2447–2458.
17. **Miller, J. H.** 1972. Experiments in molecular genetics. Cold Spring Harbor Laboratory, Cold Spring Harbor, N.Y.
18. **Nakamoto, R. K.** 1996. Mechanisms of active transport in the F_oF_1 ATP synthase. J. Membr. Biol. **151:**101–111.
19. **Nielsen, J., F. G. Hansen, J. Hoppe, P. Friedl, and K. von Meyenburg.** 1981. The nucleotide sequence of the *atp* genes coding for the F_o subunits a, b, c, and the F_1 subunit δ of the membrane bound ATP synthase of *Escherichia coli*. Mol. Gen. Genet. **184:**33–39.
20. **Patel, A., and S. D. Dunn.** 1992. RNase E-dependent cleavages in the 5′ and 3′ regions of the *Escherichia coli unc* mRNA. J. Bacteriol. **174:**3541–3548.
21. **Patel, A., and S. D. Dunn.** 1995. Degradation of the *Escherichia coli uncB* mRNA by multiple endonucleolytic cleavages. J. Bacteriol. **177:**3917–3922.
22. **Schaefer, E. M., D. Hartz, L. Gold, and R. D. Simoni.** 1989. Ribosome-binding sites and RNA processing sites in the transcript of the *Escherichia coli unc* operon. J. Bacteriol. **171:**3901–3908.
23. **Senior, A. E.** 1990. The proton-translocating ATPase of *Escherichia coli*. Annu. Rev. Biophys. Biophys. Chem. **19:**7–41.
24. **Silhavy, T. J., M. L. Berman, and L. W. Enquist.** 1984. Experiments with gene fusions. Cold Spring Harbor Laboratory, Cold Spring Harbor, N.Y.
25. **Solomon, K. A., D. K. W. Hsu, and W. S. A. Brusilow.** 1989. Use of *lacZ* fusions to measure in vivo expression of the first three genes of the *Escherichia coli unc* operon. J. Bacteriol. **171:**3039–3045.
26. **Stormo, G. D., T. D. Schneider, L. Gold, and A. Ehrenfeucht.** 1982. Use of the 'Perceptron' algorithm to distinguish translational initiation sites in *E. coli*. Nucleic Acids Res. **10:**2997–3011.
27. **Vik, S. B., and B. J. Antonio.** 1994. A mechanism of proton translocation by F_1F_o ATP synthases suggested by double mutants of the a subunit. J. Biol. Chem. **269:**30364–30369.
28. **von Meyenburg, K., B. B. Jørgensen, O. Michelsen, L. Sørensen, and J. E. G. McCarthy.** 1985. Proton conduction by subunit a of the membrane-bound ATP synthase of *Escherichia coli* revealed after induced overproduction. EMBO J. **4:**2357–2363.
29. **Wada, K., S. Aota, R. Tsuchiya, F. Ishibashi, T. Gojobori, and T. Ikemura.** 1990. Codon usage tabulated from the GenBank genetic sequence data. Nucleic Acids Res. **18:**2367–2368.
30. **Zuker, M.** 1989. On finding all suboptimal foldings of an RNA molecule. Science **244:**48–52.